

Exploration of $SU(N_c)$ gauge theory with many Wilson fermions at strong coupling

Kei-ichi Nagai, Georgina Carrillo-Ruiz, Gergana Koleva, Randy Lewis

Department of Physics and Astronomy, York University, Toronto, Canada, M3J 1P3

Abstract

We explore aspects of the phase structure of $SU(2)$ and $SU(3)$ lattice gauge theories at strong coupling with many flavours N_f of Wilson fermions in the fundamental representation. The pseudoscalar meson mass as a function of hopping parameter is observed to deviate from the expected analytic dependence, at least for sufficiently large N_f . Implications of this effect are discussed, including the relevance to recent searches for an infrared fixed point.

PACS numbers: 11.5.15.Ha

1. Introduction

There has been a lot of interest recently in identifying an infrared fixed point, and the possibility of an associated conformal window, for $SU(N_c)$ gauge theories as a function of the number of fermion flavours N_f [1, 2, 3, 4, 5, 6, 7, 8, 9], motivated by the pioneering work of Banks and Zaks[10]. For a valuable review, see Ref. [11]. Much of the interest stems from the longstanding suggestion that a (nearly) conformal gauge theory could play a key role in electroweak symmetry breaking beyond the standard model of particle physics[12, 13, 14]. For fermions in the fundamental representation, the prediction obtained from a detailed study using the Wilson fermion action[1] differs from subsequent studies that use other actions[11]. According to Ref. [15] it is generally believed that confinement exists in the strong coupling limit for any N_f ; the disagreement with data from the Wilson action[1] suggests that the unphysical Wilson term has a dramatic effect. In the present work, we revisit the strong coupling limit of the Wilson action with the goal of providing some additional insight into this issue.

An $SU(N_c)$ lattice gauge theory with fundamental Wilson fermions is expected to have a phase where flavour and parity are spontaneously broken, known as the Aoki phase[16, 17]. The expected phase diagram (for example figure 3 of Ref. [17]) is sketched in the plane spanned by the two relevant parameters: the gauge coupling and the fermion mass. The weak coupling part of the diagram shows “fingers” of Aoki phase separated by regions of symmetric phase, but ongoing research by various groups is refining this picture for specific discretizations and lattice improvement scenarios[18, 19, 20, 21, 22, 23, 24]. The strong coupling part of the original expected phase diagram is simpler: the Aoki phase exists for quark masses of smaller magnitude and the symmetric phase exists for quark masses of larger magnitude. In the extreme strong coupling limit ($g = \infty$), the phase boundary is predicted to be at a specific critical value of the hopping parameter,

$$\kappa_c = \frac{1}{4}. \quad (1)$$

Recall that the hopping parameter κ is related to the dimensionless bare fermion mass m_0 as follows:

$$\kappa \equiv \frac{1}{2m_0 + 8}. \quad (2)$$

In addition, the dimensionless pion mass in the strong coupling limit is predicted to be a rather simple function of the hopping parameter[16],

$$\cosh(m_\pi) = 1 + \frac{(1 - 16\kappa^2)(1 - 4\kappa^2)}{8\kappa^2(1 - 6\kappa^2)}. \quad (3)$$

This expression for the pion mass was derived long ago for quenched configurations (i.e. $N_f = 0$ inside the configurations)[25, 26], and initial tests of its validity for $N_f > 0$ were

presented in some of the direct numerical simulations within Ref. [1]. A central result of our work is the observation of systematic deviations from Eq. (3) in exploratory simulations with multiple Wilson fermions at $\beta = 0$.

2. Simulation details

For this study we use the standard plaquette gauge action and the standard Wilson fermion action for each of the N_f degenerate fermions,

$$S = S_G + \sum_{f=1}^{N_f} S_W^f, \quad (4)$$

$$S_G = \frac{\beta}{2} \sum_{x,\mu,\nu} \left(1 - \frac{1}{N_c} \text{ReTr} U_\mu(x) U_\nu(x+\mu) U_\mu^\dagger(x+\nu) U_\nu^\dagger(x) \right), \quad (5)$$

$$S_W^f = \sum_x \left[\bar{\psi}^f(x) \psi^f(x) - \kappa \left\{ \bar{\psi}^f(x) (1 - \gamma_\mu) U_\mu(x) \psi^f(x+\mu) + \bar{\psi}^f(x+\mu) (1 + \gamma_\mu) U_\mu^\dagger(x) \psi^f(x) \right\} \right], \quad (6)$$

where $\beta = 2N_c/g^2$ with g the gauge coupling, and where $U_\mu(x)$ is the $SU(N_c)$ -valued link variable. Then the partition function Z is

$$\begin{aligned} Z &= \int [dU_\mu(x)] \prod_{f=1}^{N_f} [d\bar{\psi}^f(x)] [d\psi^f(x)] \exp(-S) \\ &= \int [dU_\mu(x)] \left(\det(D_W^\dagger D_W) \right)^{\frac{N_f}{2}} \exp(-S_G), \end{aligned} \quad (7)$$

where D_W is the kernel of the single-fermion action $S_W^f = \bar{\psi}^f(x) D_W(x, y) \psi^f(y)$.

Simulations are performed with a standard Hybrid Monte Carlo (HMC). For independent confirmation, simulations for the heavier fermions are repeated using a Polynomial Hybrid Monte Carlo (PHMC)¹. In each Molecular Dynamics (MD) evolution, the number of steps per trajectory N_{MD} is tuned to beyond 80% acceptance for the Metropolis test. The step size $\Delta\tau$ is defined by $\Delta\tau N_{\text{MD}} = 1$.

Our simulations focus primarily on $\beta = 0$, but some studies at $\beta = 2$ will also be reported. Lattice sizes include $6^2 \times 12^2$, $8^2 \times 16^2$, $12^2 \times 24^2$ and $12^3 \times 24$. With zero temperature simulations in mind, we use periodic boundary conditions and define the Euclidean time dimension to be greater than or equal to every spatial dimension. For each chosen set of parameters, 50 to 100 configurations were collected after thermalization, with 4 or 5 trajectories between saved configurations.

¹Use of our PHMC for the lighter fermions would require a polynomial of remarkably high degree.

Our primary observables are the average plaquette $\langle \square \rangle$, the pseudoscalar meson mass m_π , and the axial-Ward-Takahashi-identity quark mass m_q^{AWI} , all defined in standard fashion:

$$\langle \square \rangle = \left\langle \frac{1}{12N_c V} \sum_{x,\mu,\nu} \text{ReTr} U_\mu(x) U_\nu(x+\mu) U_\mu^\dagger(x+\nu) U_\nu^\dagger(x) \right\rangle, \quad (8)$$

$$\left\langle \sum_{\mathbf{x}} P(\mathbf{x}, t) P(\mathbf{0}, 0) \right\rangle = c_\pi e^{-m_\pi t} + \sum_n c_n e^{-m_n t} \quad (\text{with } m_n > m_\pi \forall n), \quad (9)$$

$$m_q^{\text{AWI}} = \frac{\langle \nabla_4 \sum_{\mathbf{x}} A_4(\mathbf{x}, t) P(\mathbf{0}, 0) \rangle}{\langle 2 \sum_{\mathbf{x}} P(\mathbf{x}, t) P(\mathbf{0}, 0) \rangle}, \quad (10)$$

where V denotes the total number of lattice sites, ∇_4 is the symmetric temporal derivative operator, and the flavour non-singlet bilinear operators (with flavour index omitted) are

$$P(\mathbf{x}, t) = \bar{\psi}(\mathbf{x}, t) \gamma_5 \psi(\mathbf{x}, t), \quad (11)$$

$$A_4(\mathbf{x}, t) = \bar{\psi}(\mathbf{x}, t) \gamma_4 \gamma_5 \psi(\mathbf{x}, t). \quad (12)$$

3. $SU(2)$ with many flavours at $\beta = 0$

For a first indication of the difference between quenched and dynamical simulations, consider the average plaquette for various numbers of flavours, as shown in Fig. 1. An abrupt transition is clearly seen for $N_f \geq 6$, with a two-state signal defining the transition region in each case. The data at $N_f = 4$ hint at a transition but are not conclusive, though other observables to be discussed below will confirm a $N_f = 4$ transition. At $N_f = 2$ the transition is either suppressed or absent. This behaviour implies the existence of a first order transition for sufficiently large N_f , and was already reported for the $SU(3)$ case in Ref. [1] and for $SU(2)$ with two flavours of adjoint-representation fermions in Refs. [2, 8]. Our results show that the first order transition moves to larger values of $1/\kappa$ as N_f is increased. All of our observed transitions are in the range $1/8 < \kappa < 1/4$.

Fig. 2 shows m_π^2 and m_q^{AWI} over a wide range of $1/\kappa$. Notice that m_π^2 and m_q^{AWI} become insensitive to N_f as $1/\kappa$ increases. This is no surprise because sufficiently heavy quarks have a minimal effect on the vacuum structure of the theory, so meson and quark masses for any $N_f > 0$ approach their quenched ($N_f = 0$) values as $1/\kappa$ grows.

A close-up of the small $1/\kappa$ region is displayed in Fig. 3. The same transition that was observed in the elementary plaquette is clearly seen in m_π^2 and m_q^{AWI} as well. From these data it is clear that the transition exists at least for $N_f \geq 4$ and the two-state

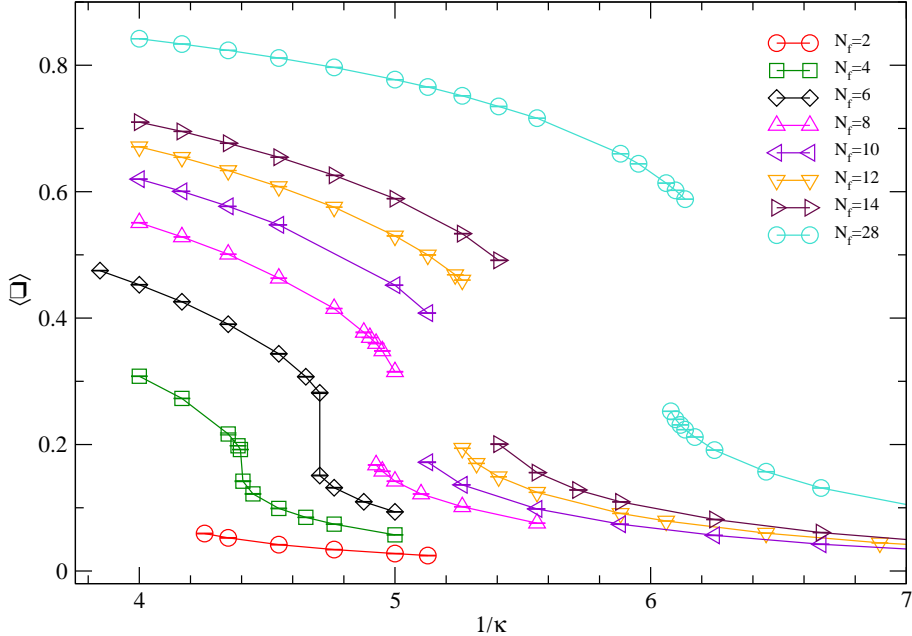


Figure 1: Average plaquette as a function of $1/\kappa$ in $SU(2)$ gauge theory with N_f flavours at $\beta = 0$.

signals imply that it is first order at least for $N_f \geq 6$. The transition moves to larger $1/\kappa$ as N_f is increased and we speculate that the transition will approach $\kappa = 1/8$ as $N_f \rightarrow \infty$, i.e. the gauge theory with infinitely many fermions will become the free theory.

It should be noted that Fig. 1 is obtained for all four of our lattice volumes: no volume dependence is observed. This was expected in advance because the average plaquette is a short distance quantity. We have similarly confirmed volume independence for m_π^2 and m_q^{AWI} over our range of volumes, and examples are presented in Fig. 4. In particular, the transition shows no evidence of vanishing in the infinite volume limit, and it shows no evidence of moving to $\kappa = 1/4$ in the infinite volume limit.

Besides the transition itself, Figs. 3 and 4 show an interesting curvature at values of $1/\kappa$ above the transition, where the slope deviates more and more from the quenched slope when approaching the transition point. If someone wanted to extrapolate to $m_\pi^2 = 0$ using only data above the transition, then the critical hopping parameter so obtained, let's name it κ_c^{ext} , would be smaller than $1/4$. Of particular interest is the fact that even the data above the transition in Figs. 3 and 4 do not follow Eq. (3) and do not arrive at $\kappa_c^{\text{ext}} = 1/4$ despite Eq. (1).

To ascertain the properties of the transition and of the regions it separates, a range of other observables should be discussed. That discussion goes beyond the scope of the present work, but brief comments and selected plots can be found in Appendix A.

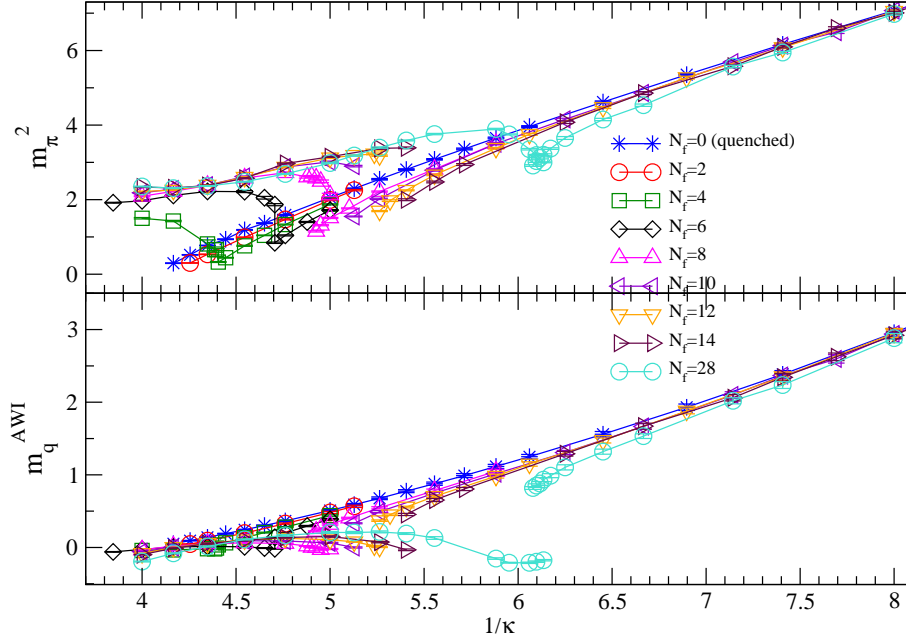


Figure 2: m_π^2 and m_q^{AWI} as functions of $1/\kappa$ in $SU(2)$ gauge theory with N_f flavours at $\beta = 0$.

4. $SU(3)$ with many flavours at $\beta = 0$

Qualitatively the situation for $SU(3)$ is similar to that for $SU(2)$, but our quantitative results indicate that deviations from Eq. (3) are smaller for $SU(3)$. Perhaps a large- N_c suppression mechanism is at work. Data for the average plaquette, pseudoscalar meson mass, and axial-Ward-Takahashi-identity quark mass are plotted in Figs. 5 and 6. Notice that m_π^2 is consistent with Eq. (3) for $N_f = 0$, but the $N_f > 0$ data display bending that is very similar to the $SU(2)$ case but of smaller magnitude.

The search for a possible transition is more expensive for $SU(3)$ than for $SU(2)$ because we must work at larger κ . A transition is found to exist for $N_f \geq 8$ but we cannot say whether it is abrupt. Recall that Ref. [1] found the transition to occur only for $N_f \geq 7$; they rely to some extent on counting the conjugate gradient iterations required during thermalization to determine the phase for $N_f = 6$ at $\kappa = 1/4$. (We comment briefly in Appendix B.) Our results² do show hints of a transition for $N_f = 6$.

²The configurations of $N_f = 6$ at $\kappa = 0.25$ in our case are generated from the last configuration of $N_f = 8$ at $\kappa = 0.25$. We use the HMC algorithm with a time step of $\Delta\tau = 0.005$, while Ref. [1] uses the approximate R algorithm with $\Delta\tau = 0.01$.

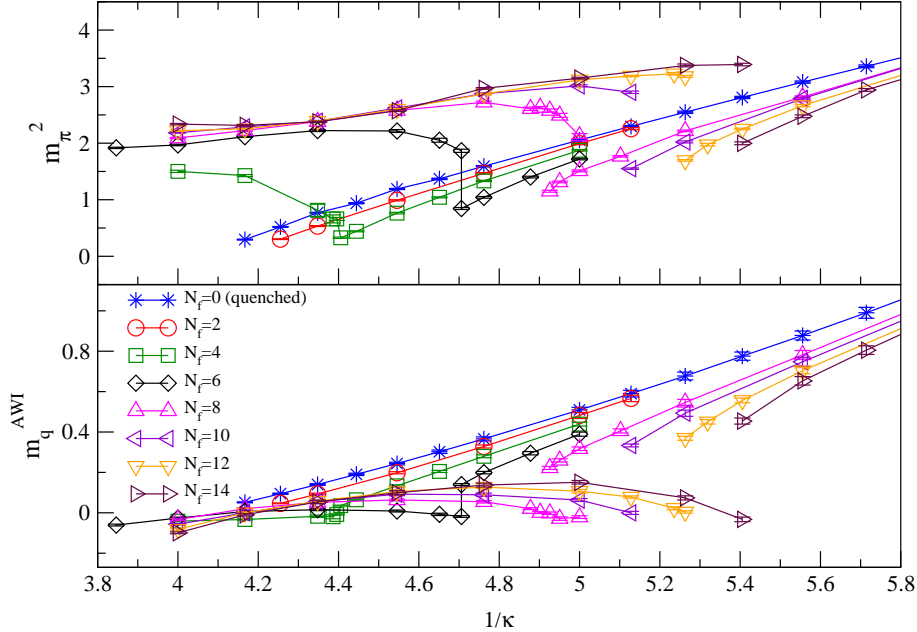


Figure 3: Same as Figure 2 but for a smaller range of $1/\kappa$.

5. Discussion

Simulations on small space-time lattices in the strong coupling limit display the phase transition already discussed in Ref. [1], but the present work makes the additional observation that the dependence of the pseudoscalar meson mass on the hopping parameter deviates from the expected formula, Eq. (3), as seen in Figs. 4 and 6. These deviations, which appear as bending in plots of meson (and quark) mass versus hopping parameter, are easily seen for $N_c = 2$ and are smaller but still observed for $N_c = 3$. The formula in Eq. (3) was derived through a large- N_c expansion[16], and the present data for $N_c = 2, 3$ suggest a rather rapid approach to Eq. (3) as N_c is increased. Eq. (3) is also obtained for any N_c with $N_f = 0$.

Because of the phase transition there is generally no value of the hopping parameter at which the pseudoscalar meson becomes massless, but extrapolation from above the phase transition (i.e. from smaller hopping parameters) does allow the definition of an effective critical hopping parameter, $\kappa_c^{\text{ext}}(N_f)$. This extrapolated value is found to obey

$$\kappa_c^{\text{ext}}(N_f) < \kappa_c^{\text{ext}}(N_f - 1) < \dots < \kappa_c^{\text{ext}}(1) < \kappa_c^{\text{ext}}(0) = \frac{1}{4} \quad (13)$$

as a consequence of the observed deviation away from Eq. (3).

The authors of Ref. [1] performed a detailed study of $SU(3)$ gauge theory with N_f Wilson fermions and from that study they proposed a phase structure with regions of confinement and deconfinement for certain values of N_f . They also include a brief

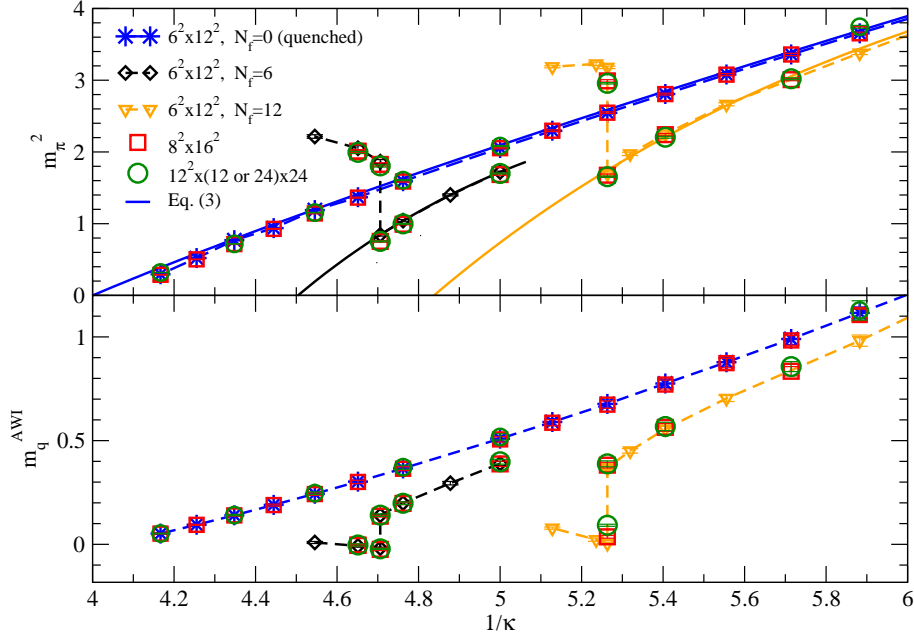


Figure 4: Volume independence of m_π^2 and m_q^{AWI} as a function of $1/\kappa$ in $SU(2)$ gauge theory for $N_f = 6$ and 12 at $\beta = 0$. The prediction from Eq. (3) is shown as a solid blue curve that reaches $m_\pi^2 = 0$ at $1/\kappa = 4$. Quadratic fits to lattice data for m_π^2 are shown as a pair of solid curves ($N_f = 6$ is black and $N_f = 12$ is orange).

appendix (in the most recent publication in [1]) devoted to the $SU(2)$ theory, where $\kappa_c = 1/4$ is assumed and simulations at that hopping parameter are used as the basis for conclusions about a confinement/deconfinement transition. The results of Ref. [1] differ from those obtained using other actions[11], and one might ask whether assumptions about $\kappa_c = 1/4$ might play a role. However, Eq. (13) confirms that for any N_f

$$\kappa_d(N_f) < \kappa_c^{\text{ext}}(N_f) \leq \frac{1}{4}, \quad (14)$$

where κ_d is the location of the phase transition; this fact is sufficient to leave the conclusions of Ref. [1] intact. Therefore the source of discrepancies between the phase structure obtained from the Wilson action versus other actions must be sought elsewhere.

It is worth noting that phenomena in the strong coupling limit are not typical of results at weaker couplings. For example the average plaquette, meson mass, and quark mass for the $SU(2)$ theory at $\beta = 2$ are plotted in Figs. 7 and 8. Instead of an abrupt transition that is essentially independent of lattice volume, we now see smoothly continuous functions and the meson mass has a significant volume dependence. Detailed studies at $\beta \neq 0$ are left for future work.

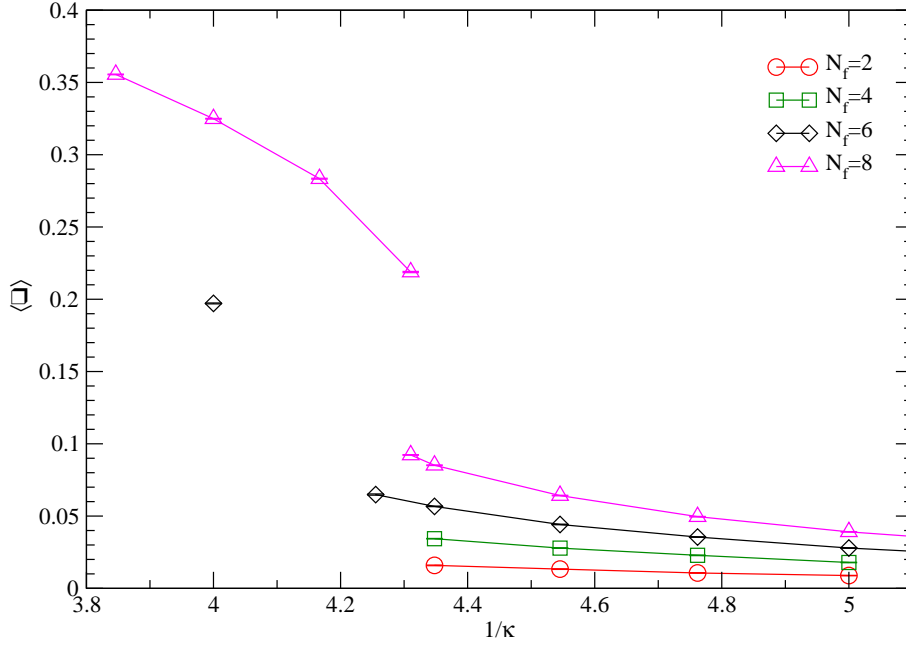


Figure 5: Average plaquette as a function of $1/\kappa$ in $SU(3)$ gauge theory with N_f flavours at $\beta = 0$.

Appendix A: Additional observables

A Polyakov loop is the trace of a product of links in a straight line along a lattice axis which, via periodic boundary conditions, closes upon itself. Polyakov loops are often used as an indicator for confinement. The absolute value of a Polyakov loop is plotted in Fig. 9 at $\beta = 0$ on $6^2 \times 12^2$ lattices. For each of the two cases $N_f = 6$ and $N_f = 8$, the graph shows the Polyakov loops in both the shorter ($N_x = 6$) and longer ($N_t = 12$) lattice directions. The shorter Polyakov loops are numerically large and dependent on the hopping parameter, with a two-state signal at the transition for large enough N_f . The longer Polyakov loops are consistent with zero for all values of κ . We refrain from drawing conclusions about confinement from this brief consideration of Polyakov loops.

For discussions of chiral symmetry and its possible breaking, natural quantities include the chiral condensate $\langle \bar{\psi}\psi \rangle$ and the pseudoscalar density $\langle \bar{\psi}\gamma_5\psi \rangle$. The low-lying eigenvalues of the Wilson-Dirac operator relate to these observables through the spectral representation of the quark propagator. For instance, $\langle \bar{\psi}\gamma_5\psi \rangle = \sum_{\lambda} \frac{\langle \lambda | \lambda \rangle}{\lambda(H_W)}$ and $\langle \bar{\psi}\psi \rangle = \sum_{\lambda} \frac{\langle \lambda | \gamma_5 | \lambda \rangle}{\lambda(H_W)}$, where $\lambda(H_W)$ and $|\lambda\rangle$ are an eigenvalue and eigenvector respectively of the hermitian Wilson-Dirac operator $H_W = \gamma_5 D_W$.

The upper panel of Fig. 10 is the lowest eigenvalue, μ , defined by $\mu = \sqrt{\lambda_0(H_W^2)}$ in the eigenvalue equation, $H_W^2 |\lambda_0\rangle = \lambda_0 |\lambda_0\rangle$, and obtained by the Ritz functional method. This behaviour hints at the dependence $\langle \bar{\psi}\gamma_5\psi \rangle \sim 1/\mu$. At least for $N_f \geq 4$,

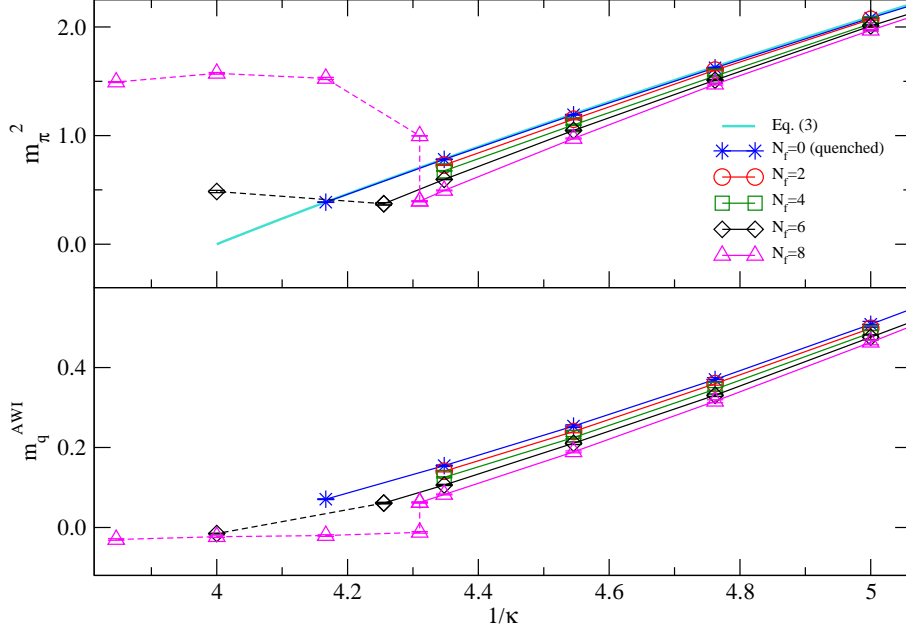


Figure 6: m_π^2 and m_q^{AWI} as functions of $1/\kappa$ in $SU(3)$ gauge theory with N_f flavours at $\beta = 0$. The prediction from Eq. (3) is shown as a solid blue curve reaching $m_\pi^2 = 0$ at $1/\kappa = 4$.

two phases are found and in both phases the eigenvalues are not particularly small.

Because Wilson fermions break chiral symmetry explicitly, the chiral condensate is not adequate and should be replaced by the subtracted chiral condensate defined by $(\bar{\psi}\psi)_{\text{subt}} = 2m_q^{\text{AWI}}\mathcal{N}$ where $\mathcal{N} = (2\kappa)^2 \sum_{\mathbf{x},t} \langle P(\mathbf{x},t)P(\mathbf{0},0) \rangle$. The fermion mass m_q^{AWI} itself is discussed in the main body of this article, and it is most naturally defined only for $1/\kappa$ values above the transition, so here we focus on the observation of \mathcal{N} . The lower panel of Fig. 10 displays \mathcal{N} for $SU(2)$ gauge theory at strong coupling for various N_f . Indications of a $1/m_q$ divergence in the confinement phase (i.e. $1/\kappa$ above the transition) are visible, as expected. For both observables in Fig. 10, the transition is visible when $N_f \geq 4$.

Appendix B: Algorithmic issues

The HMC algorithm uses a number of trajectories, traditionally distinguished by an integer τ . Each trajectory uses some number of molecular dynamics steps, N_{MD} , and each of those uses some number of Conjugate Gradient (CG) iterations, $n_i^{\text{CG}}(\tau)$ with $1 \leq i \leq N_{\text{MD}}$, to attain the imposed precision. The average number of CG iterations per MD step is therefore $N_{\text{CG}}(\tau) = \frac{1}{N_{\text{MD}}} \sum_{i=1}^{N_{\text{MD}}} n_i^{\text{CG}}(\tau)$. The left panel of Fig. 11 shows

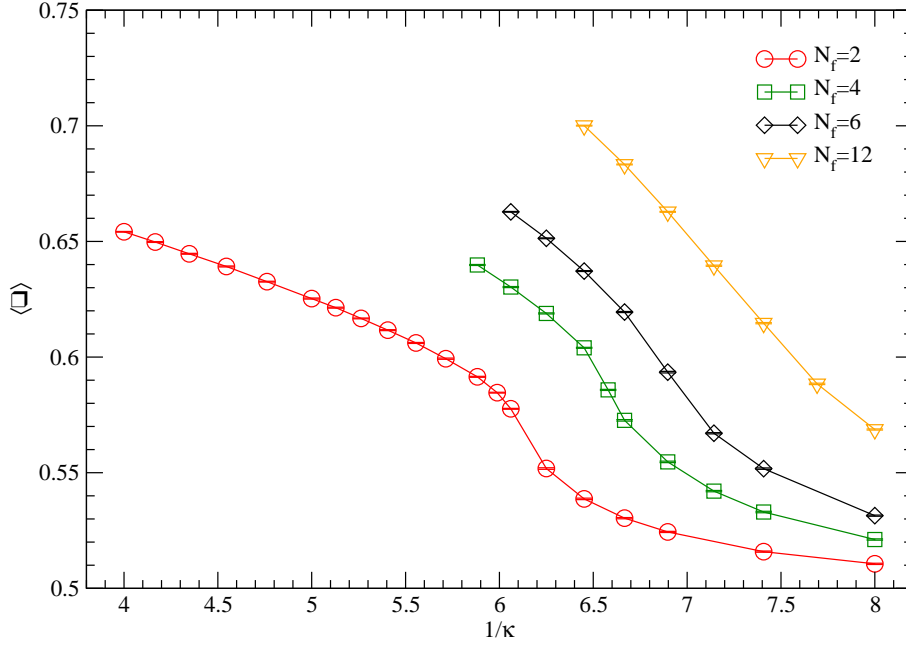


Figure 7: Average plaquette as a function of $1/\kappa$ in $SU(2)$ gauge theory with N_f flavours at $\beta = 2$ on $8^2 \times 16^2$ lattices.

this quantity for sequential trajectories during thermalization for $SU(2)$ with $N_f = 6$, $\beta = 0$, and $\kappa = 0.215$ on a $8^2 \times 16^2$ lattice with precision defined by $\|r_{CG}^{res}\| < 10^{-12}$. For reference, the average plaquette is also plotted for each trajectory. The hot start requires more trajectories before reaching thermalization, and some of those trajectories needed many CG iterations. One could possibly be tempted to abort such a calculation before reaching equilibrium and assume that the increasing $N_{CG}(\tau)$ would never return to a smaller value at larger τ . The right panel of Fig. 11 shows $N_{CG}(\tau)$ for $SU(3)$ at $N_f = 6$, $\beta = 0$, and $\kappa = 0.250$ on a $6^2 \times 12^2$ lattice with $\|r_{CG}^{res}\| < 10^{-12}$ and $N_{MD} = 200$. When configuration generation starts from the last configuration of $N_f = 8$ at $\kappa = 0.250$, the HMC becomes stable at 65% acceptance and $N_{CG}(\tau) = O(10^3)$. On the other hand, the hot and cold starts are not accepted by the HMC's Metropolis test with $N_{CG}(\tau) = O(10^4)$. In both cases³ of Fig. 11, the large value of $N_{CG}(\tau)$ does not imply the existence of a massless mode.

Acknowledgments

This work was supported in part by the Natural Sciences and Engineering Research Council of Canada, and was made possible by the facilities of the Shared Hierarchical

³We plotted the beginning $O(10)$ trajectories in about 300 runs.

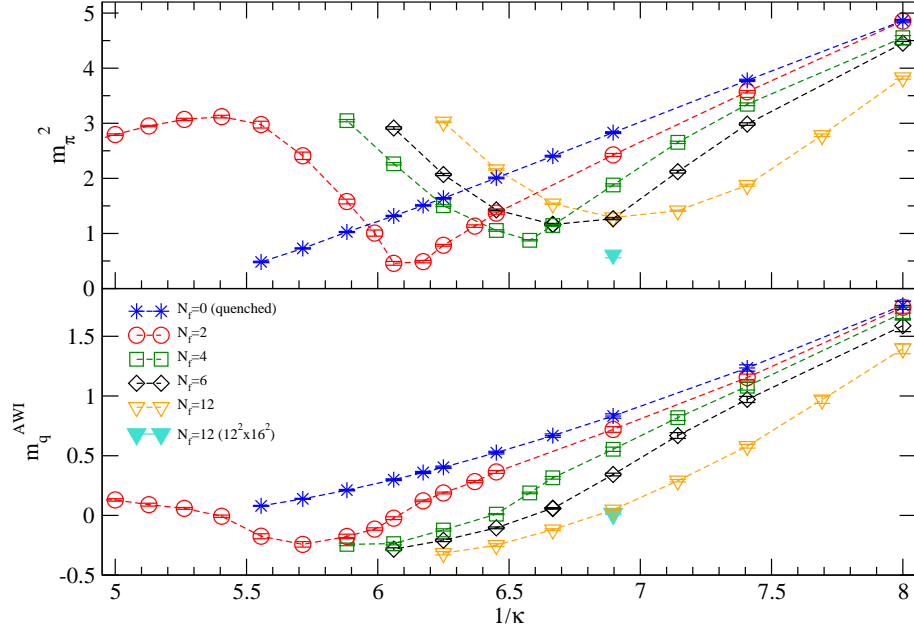


Figure 8: m_π^2 and m_q^{AWI} as functions of $1/\kappa$ in $SU(2)$ gauge theory with N_f flavours at $\beta = 2$. Lattices are $8^2 \times 16^2$ except for one point labelled as $12^2 \times 16^2$.

Academic Research Network (SHARCNET:www.sharcnet.ca). G.K. thanks the University of Regina for hospitality during her stay there, and we acknowledge use of Regina's VXRACK computer cluster.

References

- [1] Y. Iwasaki, K. Kanaya, S. Sakai and T. Yoshie, Phys. Rev. Lett. **69**, 21 (1992) and Y. Iwasaki, K. Kanaya, S. Kaya, S. Sakai and T. Yoshie, Phys. Rev. D **54**, 7010 (1996) [arXiv:hep-lat/9605030] and Y. Iwasaki, K. Kanaya, S. Kaya, S. Sakai and T. Yoshie, Phys. Rev. D **69**, 014507 (2004) [arXiv:hep-lat/0309159].
- [2] S. Catterall and F. Sannino, Phys. Rev. D **76**, 034504 (2007) [arXiv:0705.1664 [hep-lat]] and S. Catterall, J. Giedt, F. Sannino and J. Schneible, JHEP **0811**, 009 (2008) [arXiv:0807.0792 [hep-lat]].
- [3] T. Appelquist, G. T. Fleming and E. T. Neil, Phys. Rev. Lett. **100**, 171607 (2008) [Erratum-ibid. **102**, 149902 (2009)] [arXiv:0712.0609 [hep-ph]] and Phys. Rev. D **79**, 076010 (2009) [arXiv:0901.3766 [hep-ph]].

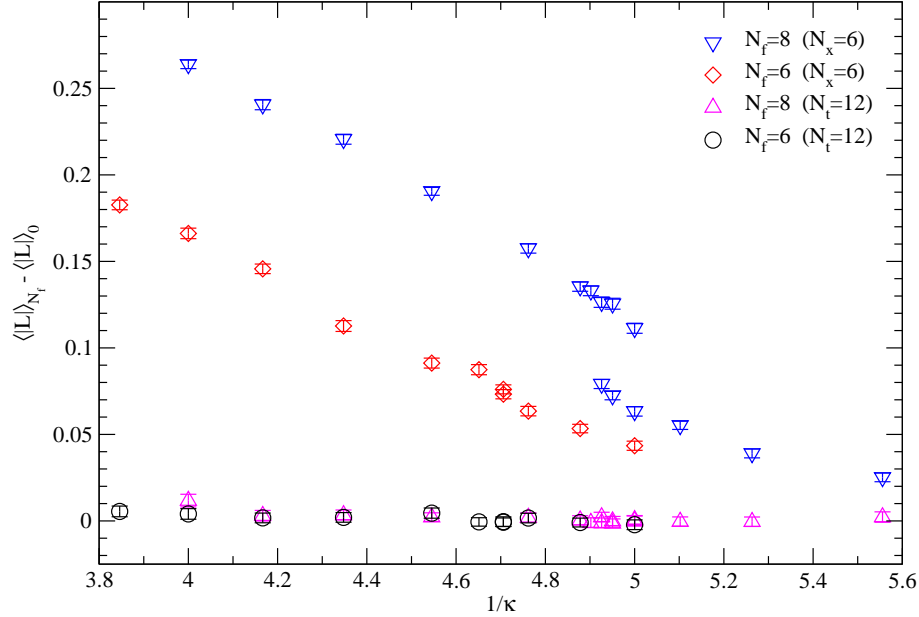


Figure 9: The dependence of a Polyakov loop $\langle |L| \rangle$ on N_f flavours is expressed through the difference $\langle |L| \rangle_{N_f} - \langle |L| \rangle_0$. This difference is plotted as a function of $1/\kappa$ in $SU(2)$ gauge theory on $6^2 \times 12^2$ lattices at $\beta = 0$ with $N_f = 6$ and 8.

- [4] Y. Shamir, B. Svetitsky and T. DeGrand, Phys. Rev. D **78**, 031502 (2008) [arXiv:0803.1707 [hep-lat]] and Phys. Rev. D **79**, 034501 (2009) [arXiv:0812.1427 [hep-lat]].
- [5] A. Deuzeman, M. P. Lombardo and E. Pallante, Phys. Lett. B **670**, 41 (2008) [arXiv:0804.2905 [hep-lat]] and arXiv:0904.4662 [hep-ph].
- [6] L. Del Debbio, A. Patella and C. Pica, arXiv:0805.2058 [hep-lat] and arXiv:0812.0570 [hep-lat].
- [7] Z. Fodor, K. Holland, J. Kuti, D. Nogradi and C. Schroeder, arXiv:0809.4888 [hep-lat] and arXiv:0809.4890 [hep-lat] and arXiv:0907.4562 [hep-lat].
- [8] A. J. Hietanen, J. Rantaharju, K. Rummukainen and K. Tuominen, JHEP **0905**, 025 (2009) [arXiv:0812.1467 [hep-lat]] and A. J. Hietanen, K. Rummukainen and K. Tuominen, arXiv:0904.0864 [hep-lat].
- [9] A. Hasenfratz, arXiv:0907.0919 [hep-lat].
- [10] T. Banks and A. Zaks, Nucl. Phys. B **196**, 189 (1982).
- [11] G. T. Fleming, PoS **LATTICE2008**, 021 (2008) [arXiv:0812.2035 [hep-lat]].

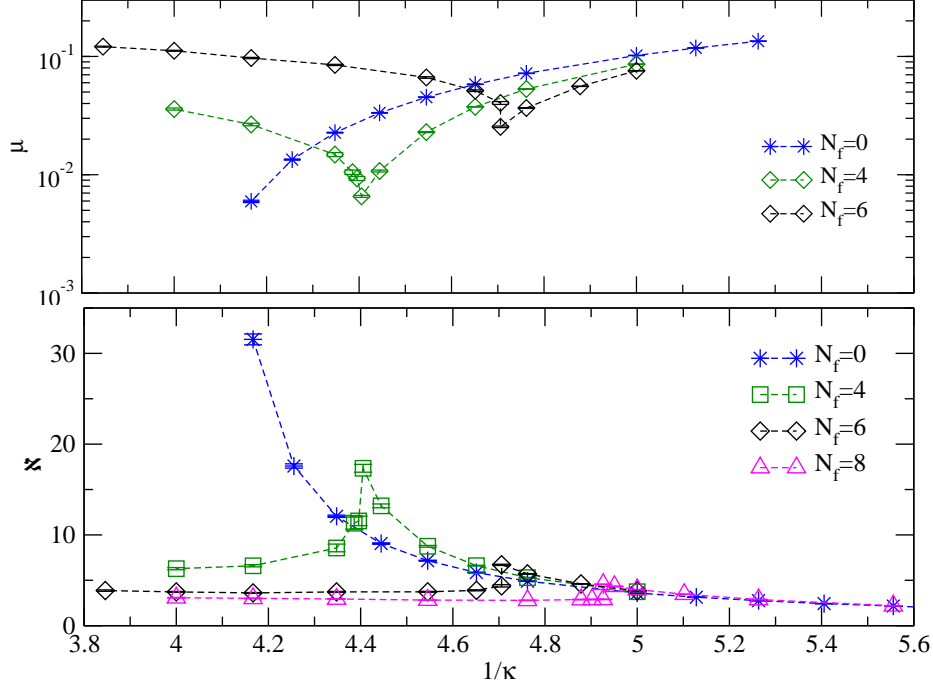


Figure 10: $SU(2)$ gauge theory with N_f flavours at $\beta = 0$ on a $6^2 \times 12^2$ lattice. Upper panel: $\mu = \sqrt{\lambda_0(H_W^2)}$, where $\lambda_0(H_W^2)$ is the lowest eigenvalue of H_W^2 , as a function of $1/\kappa$. Lower panel: $\mathcal{N} = (2\kappa)^2 \sum_{\mathbf{x},t} \langle P(\mathbf{x},t)P(0) \rangle$ as a function of $1/\kappa$.

- [12] B. Holdom, Phys. Rev. D **24**, 1441 (1981) and Phys. Lett. B **150**, 301 (1985).
- [13] K. Yamawaki, M. Bando and K.-i. Matumoto, Phys. Rev. Lett. **56**, 1335 (1986).
- [14] T. Appelquist and L. C. R. Wijewardhana, Phys. Rev. D **35**, 774 (1987) and Phys. Rev. D **36**, 568 (1987).
- [15] T. DeGrand and A. Hasenfratz, arXiv:0906.1976 [hep-lat].
- [16] S. Aoki, Phys. Rev. D **30**, 2653 (1984) and S. Aoki, Phys. Rev. Lett. **57**, 3136 (1986).
- [17] S. Aoki, Prog. Theor. Phys. Suppl. **122**, 179 (1996) [arXiv:hep-lat/9509008].
- [18] F. Farchioni *et al.*, Eur. Phys. J. C **39**, 421 (2005) [arXiv:hep-lat/0406039].
- [19] C. Michael and C. Urbach [ETM Collaboration], PoS **LAT2007** (2007) 122 [arXiv:0709.4564 [hep-lat]].
- [20] Ph. Boucaud *et al.* [ETM collaboration], Comput. Phys. Commun. **179**, 695 (2008) [arXiv:0803.0224 [hep-lat]].

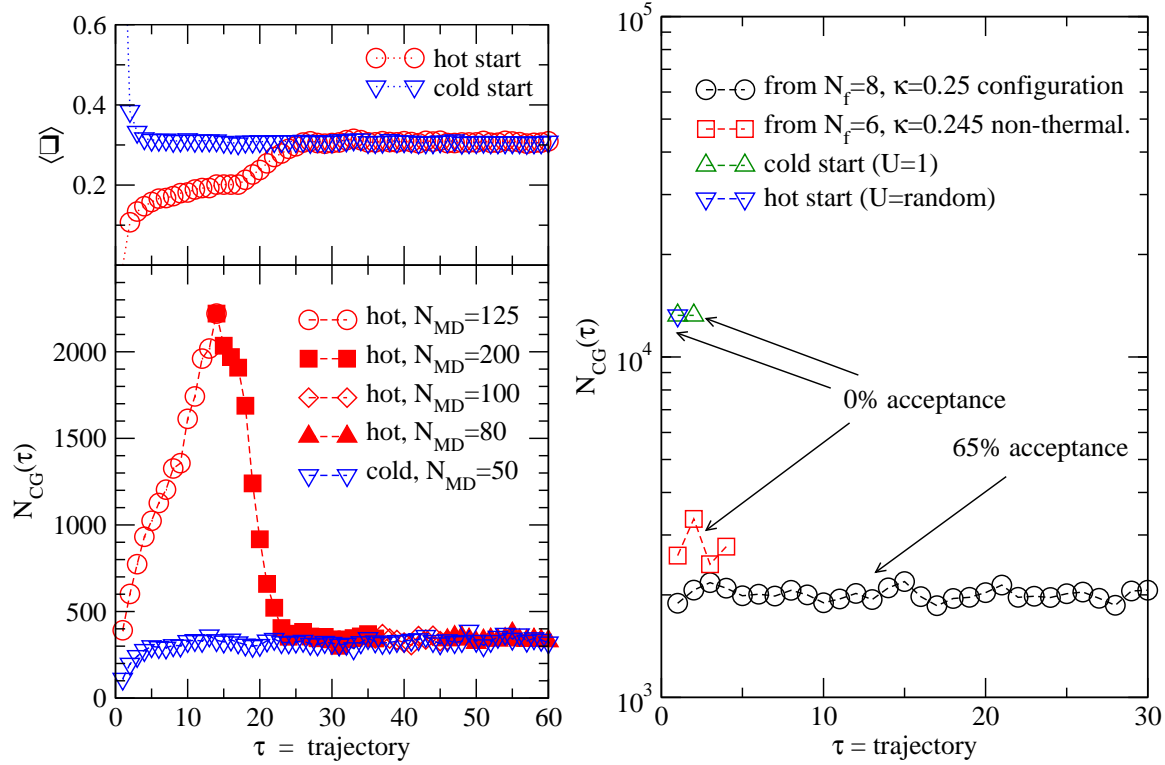


Figure 11: Left panel: The average plaquette and $N_{CG}(\tau)$ versus trajectory index τ in $SU(2)$ gauge theory on $8^2 \times 16^2$ lattice at $\beta = 0$ and $\kappa = 0.215$ with $N_f = 6$. Right panel: $N_{CG}(\tau)$ versus τ in $SU(3)$ gauge theory with $N_f = 6$ on $6^2 \times 12^2$ lattice at $\beta = 0$, $\kappa = 1/4$ and $N_{MD} = 200$.

- [21] E. M. Ilgenfritz, W. Kerler, M. Muller-Preussker, A. Sternbeck and H. Stuben, Phys. Rev. D **69**, 074511 (2004) [arXiv:hep-lat/0309057].
- [22] F. Farchioni *et al.*, PoS **LAT2005**, 033 (2006) [arXiv:hep-lat/0509036].
- [23] V. Azcoiti, G. Di Carlo and A. Vaquero, Phys. Rev. D **79**, 014509 (2009) [arXiv:0809.2972 [hep-lat]].
- [24] S. R. Sharpe, Phys. Rev. D **79**, 054503 (2009) [arXiv:0811.0409 [hep-lat]].
- [25] K. G. Wilson, in *New Phenomena in Subnuclear Physics*, Proceedings of the 1975 International School of Subnuclear Physics, Erice, 1975, edited by A. Zichichi (Plenum, New York, 1977).
- [26] N. Kawamoto, Nucl. Phys. B **190**, 617 (1981).